Takayasu's arteritis of the aortic arch: endovascular treatment and correlation with positron emission tomography.

J Théron and J L Tyler

AJNR Am J Neuroradiol 1987, 8 (4) 621-626
http://www.ajnr.org/content/8/4/621

Takayasu's Arteritis of the Aortic Arch: Endovascular Treatment and Correlation with Positron Emission Tomography

Jacques Théron[1]
Jane L. Tyler

A case is presented in which three arterial stenoses and one arterial occlusion due to Takayasu's disease were treated by an endovascular approach. The endovascular technique is discussed, and the clinical and angiographic findings after treatment are correlated with cerebral hemodynamic and metabolic parameters as measured by positron emission tomography.

Takayasu's arteritis is a chronic inflammatory arteriopathy of unknown origin, affecting the aorta and its main branches [1]. The inflammatory process results in fibrosis and thickening of the arterial walls, and eventual constriction or total occlusion of the vessel lumina. To date, surgical treatment of these vessels has had only limited success. We report a case of advanced Takayasu's arteritis treated successfully by the endovascular approach, in which cerebral hemodynamic and metabolic parameters were studied with positron emission tomography (PET) before and after treatment.

Case Report

A 39-year-old woman presented with acute onset of dysesthesia and weakness of the left upper extremity. Five years previously, she had suffered an ischemic episode involving the right arm; she subsequently complained of pain in the extremity and was treated symptomatically with a cervical sympathectomy. Review of her charts revealed that her right radial and brachial pulses had not been palpable since that episode.

At the time of her present admission, bilateral carotid artery bruits were audible, more intensely on the right. Again, the right brachial and radial pulses were not palpable. The neurologic examination revealed hyperreflexia and distal paresis of the left upper limb. The muscular strength in the left upper extremity was 0/5 for the extensor and flexor muscle groups, and 2/5 for the supinator and pronator muscles of the forearm. Muscle strength was normal in other groups tested. Laboratory examinations were unremarkable. CT scans of the head showed a right posterior parietal hypodensity consistent with a cerebral infarction (Fig. 1). Digital angiography demonstrated narrow stenoses at the origins of the right common carotid, the left common carotid, and the left vertebral arteries, the latter originating from the aortic arch (Fig. 2). There was also occlusion of the origin of the left external carotid artery and of the right subclavian artery. On the late phase of the angiogram, a subclavian steal phenomenon was demonstrated, with retrograde filling of the right vertebral artery and opacification of the right subclavian artery distal to the occlusion. A selective intracranial angiographic series, performed by injection of the right common carotid artery, showed no abnormalities. The diagnosis of Takayasu's arteritis was made on the basis of the patient's age and the location and number of stenoses and occlusions of the arch vessels. The patient's neurologic findings remained stable after the acute event.

The patient underwent two percutaneous endovascular treatments, 1 week apart; the first was performed 10 days after the acute event. This treatment included angioplasty of the origins of the right and left common carotid arteries and of the origin of the left vertebral artery, and a recanalization with angioplasty of the right subclavian artery. On the postprocedure arch angiographic series (Fig. 3), a marked increase was seen in the diameter of the

Received March 3, 1986; accepted after revision February 4, 1987.

Presented at the annual meeting of the American Society of Neuroradiology, San Diego, January 1986.

[1] Both authors: Brain Imaging Center, Department of Neurology and Neurosurgery, Montreal Neurological Institute and Hospital, McGill University, 3801 University Street, Montreal, P.Q., H3A 2B4, Canada. Address reprint requests to J. L. Tyler.

AJNR 8:621–626, July/August 1987
0195–6108/87/0804-0621

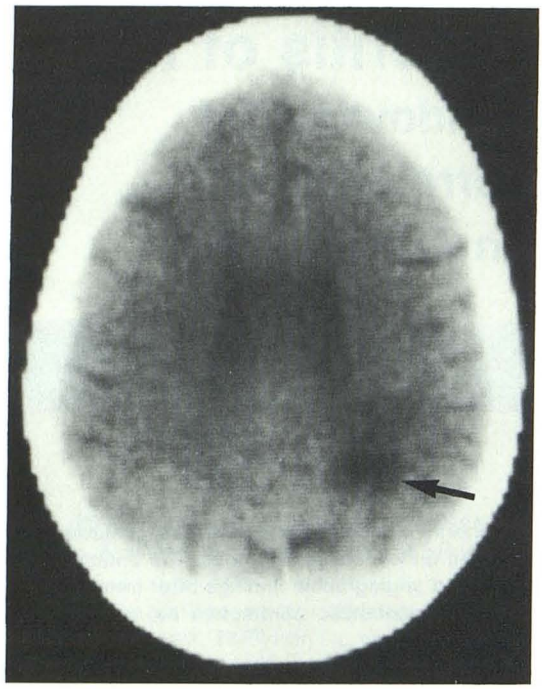

Fig. 1.—Cranial CT hypodensity (*arrow*) corresponding to infarction in right watershed area.

treated vessels, with early opacification of the right vertebral artery.

Immediately following this endovascular treatment, the patient reported a marked subjective improvement in general strength and well-being. No carotid bruits were audible, and the right radial and brachial pulses were palpable and equal to those on the left. The left upper extremity muscles gradually improved to a strength of 3/5 in the extensors and flexors, and a strength of 4/5 in the forearm pronators and supinators. The patient has been followed clinically for 18 months since the procedure and remains stable and improved.

Methodology

Endovascular Technique

At the first treatment, angioplasty of the left vertebral artery was performed via a femoral approach, using a 7-French (6 mm outside diameter, 2 cm length) angioplasty catheter (Meditech, Inc., Watertown, MA 02172). Sequentially, the balloon was inflated and then deflated; it was never left fully inflated. Angioplasty of the left common carotid artery was also performed at that time, using an 8-French (10 mm outside diameter, 3 cm length) angioplasty catheter.

A second session of endovascular treatment was performed 1 week later, and at that time angioplasty of the right common carotid artery was performed using an 8-French angioplasty catheter. Subsequently, using a 0.035-in.-diameter straight guidewire, the origin of the right subclavian artery was cannulated via the femoral approach, and an 8-French angioplasty catheter was slowly and progressively passed into the thrombosed section of the artery; dilatation of this

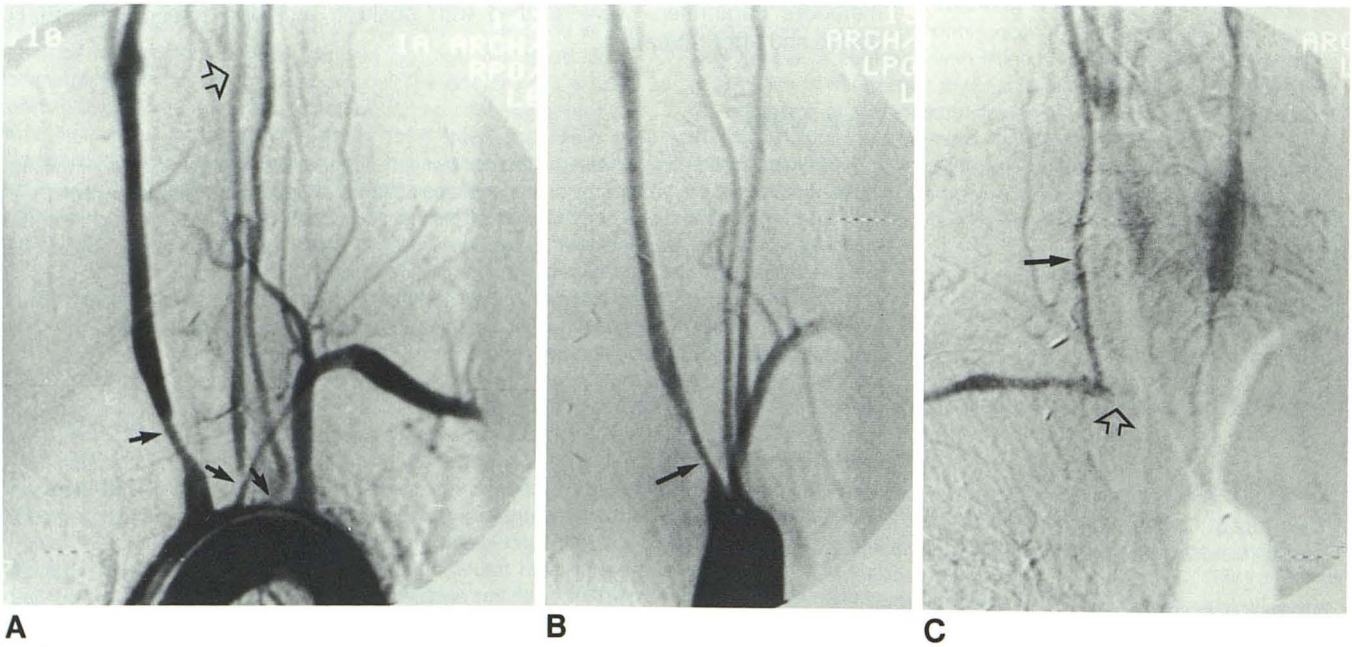

A B C

Fig. 2.—Aortic arch angiograms performed before endovascular treatment.

A, Left anterior oblique projection. Origins of right common carotid artery, left common carotid artery, and vertebral artery appear markedly narrowed (*closed arrows*). Origin of left external carotid artery (*open arrow*) appears occluded. Right subclavian artery is not opacified on this early phase.

B, Right anterior oblique projection, early phase. This series better shows narrowing of origin of right common carotid artery (*arrow*). Right subclavian artery is not opacified on these early images.

C, Right anterior projection, late phase. Retrograde filling of right vertebral artery (*closed arrow*) is seen, with late opacification of right subclavian artery distal to occlusion of its origin (*open arrow*).

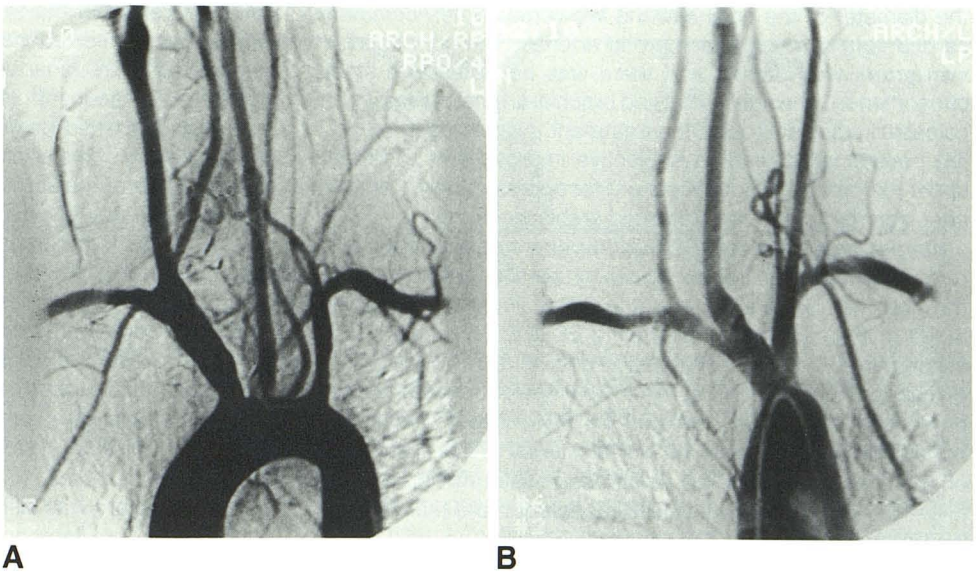

Fig. 3.—Aortic arch angiograms performed after endovascular treatment.

***A*, Left anterior oblique projection. As compared with angiogram done before treatment, diameter of treated vessels is markedly improved. There is early filling of right subclavian artery and of right vertebral artery, without steal phenomenon on late phase.**

***B*, Right anterior oblique projection. This projection better shows enlargement in diameter of right common carotid artery (compare with Fig. 1B).**

section of the vessel was accomplished by serial inflations and deflations of the catheter balloon.

During these procedures the patient received 2,000 units of heparin IV as a bolus at the time of placement of the guide catheter and subsequently 1,000 units every hour during the procedure. At the completion of the procedure, the anticoagulation was reversed with IV protamine sulfate. The patient received 325 mg of acetyl-salicylic acid orally every 6 hr for 1 day before the procedure, on the day of the procedure, and for 1 day after the procedure.

Positron Emission Tomography

PET scans were performed using the Therascan 3128 (Atomic Energy of Canada, Ltd., Ottawa, Ontario) positron tomograph [2], a two-ring scanner acquiring both direct and cross-slice coincidences simultaneously. Image resolution was 12 mm (full width at half maximum) in the transverse plane. ^{18}F-labeled fluorodeoxyglucose (FDG) was prepared in the Montreal Neurological Institute Medical Cyclotron Unit [3]. The patient received a 5 mCi bolus of IV ^{18}F-FDG over 1 min. Blood samples for determining ^{18}F plasma activity and glucose concentration were taken from the opposite arm, using direct arterial sampling. Approximately 40 min after the injection of the ^{18}F-FDG, three tomographic slices were obtained simultaneously at each of two scan positions, with the center slices located 42 mm and 62 mm, respectively, above the orbitomeatal line.

^{15}O-labeled gases, O_2, CO_2, and CO, were administered sequentially in one session to provide three separate data sets. These were combined to provide functional maps for cerebral blood flow (CBF), oxygen extraction fraction (OEF), oxygen metabolic rate ($CMRO_2$), and blood volume (CBV) [4]. OEF and $CMRO_2$ images were corrected for CBV [5].

The ^{15}O-$_2$ and ^{15}O-CO_2 gases were delivered continuously during the study period at flows of 10 mCi/min at 80 cm^3/min, and 5 mCi/min at 60 cm^3/min, respectively. Labeled gases were mixed with 200 cm^3/min of medical air, and were supplied to the patient through a plastic face mask. Once inhalation of the labeled gas was begun, equilibrium was established over a 10 min period, followed by scans at the position described for the FDG study. Typically, 1.5–2.5 million true events were recorded for each ^{15}O-O_2 image, and 2–4 million for each ^{15}O-CO_2 image.

^{15}O-CO was administered in a dose of 80 mCi/min at 100 cm^3/min for 4 min. The ^{15}O-CO was then discontinued, and after a 1 min delay, low-resolution images were obtained at the two scan positions. Typical images contained 300–500 thousand true coincidences. Throughout these studies, blood samples were obtained over 15–20 sec from an arterial line for the measurement of blood gases and plasma radioactivity.

Images were reconstructed using the Therascan standard software package [6–8]. The ^{18}F-FDG analysis program is based on the Phelps et al. [9] adaptation of the Sokoloff method [10]; a reformulation of the operational equation suggested by Brooks has been incorporated [11]. Values for gray matter rate constants and for the lumped constant were those established by Huang et al. [12]. The oxygen analysis program generates a map for each of the four functional parameters, CBF, CBV, OEF, and $CMRO_2$, for each anatomic plane as a composite data set.

Hemodynamic and metabolic parameters were measured on the day before the first angioplasty and 28 days after the second angioplasty. At the beginning of each scan, the patient's inferior orbitomeatal line was aligned with a laser line corresponding to the position of the scanner's middle slice. The patient's position was recorded at the beginning and at the end of each study to ensure accurate slice registration when comparing the various scans. The functional values obtained from cortical gray matter in the two hemispheres were compared; changes of 20% or greater were judged to be significant. Metabolic and hemodynamic values were assessed in the context of control values obtained in young healthy volunteers in this laboratory for FDG (LCMRGl mean in 20 subjects = 45.5 ± 7.7 μmol/100 g/min) and for oxygen-15 studies in 11 subjects (CBF = 50 ± 12 ml/100 g/min, CBV = 4.4 ± 0.3% brain weight, OEF = 0.42 ± 0.8, and $CMRO_2$ = 183 ± 42 μmol/100 g/min). Intrasubject variability for repeated measurements in controls was on the order of 10% for sequential FDG scans and 15–18% for repeat oxygen-15 scans.

Results

After the angioplasties and the recanalization procedure, aortic arch angiography showed a significant enlargement of

the diameter of the origins of the left vertebral, left common carotid, and right common carotid arteries. The right subclavian artery was patent, and there was no detectable steal phenomenon. The right radial and brachial arterial pulses were palpable immediately after the treatment. As previously noted, the patient felt a marked subjective improvement. The left upper extremity strength improved for approximately 1 month after treatment, and has remained stable since then.

On the preangioplasty FDG study, the cerebral metabolic rate for glucose (LCMRGl) values for cortical gray matter in the right hemisphere were at the lower limit of the normal range in this laboratory, averaging 32.9 ± 2.7 μmol/100 g tissue/min in the right hemisphere, and 35.3 ± 3.3 μmol/100 g tissue/min in the left (Fig. 4A). Twenty-eight days after the procedures, the study revealed LCMRGl values within the normal range, averaging 46.9 ± 3.0 μmol/100 g tissue/min on the right and 49.8 ± 4.0 μmol/100 g tissue/min on the left (Fig. 4B). These LCMRGl values represent more than a 40% improvement relative to the initial values.

No significant (i.e., >20%) global or hemispheric gray matter changes in OEF, CBF, CBV, or $CMRO_2$ were seen when the pre- and postangioplasty studies were compared. However, combinations of these hemodynamic and metabolic parameters (i.e., the ratios of CBF to CBV, $CMRO_2$ to LCMRGl, and LCMRGl to CBF) did demonstrate some significant findings, as shown in Table 1.

It was noted that localized significant changes were seen in the right parietal area in regions in proximity to the site of the patient's previous cerebral infarction. In this area, the follow-up metabolic studies demonstrated an 85% increase in LCMRGl, a 20% increase in oxygen extraction, a 28% decrease in cerebral blood volume, and a 20% increase in $CMRO_2$ (Table 2). Significant changes such as these were not seen in other localized cerebral regions.

Discussion

Takayasu's disease is a nonspecific obstructive arteritis, primarily involving the vessels of the aortic arch [1]. Most patients present in the second or third decades of life, with females being involved more frequently than males. The pathologic lesion is a panarteritis with initial inflammation of the adventitia, subsequent disruption and fibrotic changes in the media, and marked proliferation of the intima. The fibrosis and thickening of the arterial wall lead to stenosis or occlusion of the vessels of the aortic arch, and consequently to cerebral ischemia. Several investigators have noted the limited success of surgical treatment of Takayasu's arteritis involving the aortic arch [13, 14], with the progressive inflammatory nature of the disease resulting in a high incidence of graft occlusion. Surgery is, therefore, undertaken reluctantly.

With the advent of transluminal angioplasty [15, 16], a new technique for the treatment of this disease may be available. Two dilatations of a subclavian stenosis in a patient with Takayasu's disease have been reported previously [17, 18]. In one of these cases [17], an angioplasty of the origin of the left carotid artery was also performed using a surgical carotid arteriotomy, with temporary occlusion of the carotid during the dilatation of the stenosis. In the present case, both carotid arteries were dilated percutaneously without complication. We believe that in this type of stenosis, it is possible to perform angioplasty of the carotid arteries with relative security, because the inflammatory, nonulcerative nature of the lesions decreases the potential of embolic complications as compared with atherosclerotic stenoses [19–21].

Endovascular treatment of the subclavian steal syndrome has been reported [22–25]; however, canalization of an atherosclerotic occlusion of the subclavian artery is rarely successful [26]. We believe that the inflammatory nature of the lesions in Takayasu's arteritis makes the permanent recanalization more likely when successfully performed, as in this case.

PET provides the means to study metabolic parameters in areas of cerebral ischemia as well as in tissues adjacent to or distal from the primary areas of ischemia. Cerebral ischemia presents a difficult problem to study; even the most uniform of ischemic episodes, complete cessation of flow, can demonstrate inhomogeneous metabolic changes. The patchy per-

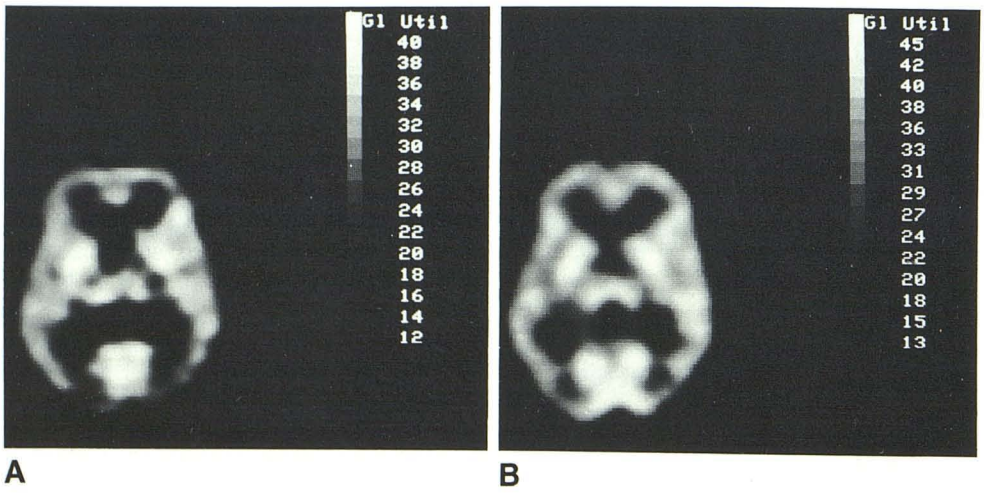

Fig. 4.—^{18}F-labeled fluorodeoxyglucose PET scans before and after endovascular treatment.

***A*, Cerebral metabolic rate for glucose in a horizontal plane 42 mm above orbitomeatal line is moderately decreased in all regions (mean = 34.1 μmol/100 g/min).**

***B*, 28 days after endovascular treatment, PET scan showed increased cerebral glucose metabolism (mean = 47.8 μmol/100 g/min).**

TABLE 1: Hemispheric Metabolic and Hemodynamic Parameters* Before and After Endovascular Treatment

Parameter	Preangioplasty		Postangioplasty		% Change	
	R	L	R	L	R	L
LCMRGl	32.9	35.3	46.9	49.8	+43	+41
CBF/CBV	8.6	7.8	9.2	9.0	+7	+15
$CMRO_2$/LCMRGl	4.66	4.54	3.28	3.24	−30	−29
LCMRGl/CBF	0.93	0.97	1.27	1.28	+37	+32

* LCMRGl (local cerebral metabolic rate for glucose) expressed as μmol/100 g/min. $CMRO_2$ (cerebral metabolic rate for oxygen) expressed as μmol/100 g tissue/min. CBV (cerebral blood volume) is expressed as a percentage of brain volume. CBF (cerebral blood flow) is expressed as ml/100 g tissue/min.

TABLE 2: Metabolic and Hemodynamic Parameters* in the Right Posterior Watershed Area

Parameter	Preangioplasty	Postangioplasty	% Change
LCMRGl	16.5	30.5	+85
CBF	28.0	34.0	+18
CBV	3.2	2.3	−28
OEF	0.35	0.42	+20
$CMRO_2$	85.8	102.5	+20
CBF/CBV	8.8	14.8	+68
$CMRO_2$/LCMRGl	5.20	3.36	−35
LCMRGl/CBF	0.59	0.90	+52

* LCMRGl (local cerebral metabolic rate of glucose) expressed as μmol/100 g tissue/min. $CMRO_2$ (cerebral metabolic rate for oxygen) expressed as μmol/100 g tissue/min. CBV (cerebral blood volume) is expressed as a percentage of brain volume. CBF (cerebral blood flow) is expressed as ml/100 g tissue/min. OEF (oxygen extraction fraction) is expressed as a percentage of 1.00.

fusion that characterizes incomplete ischemia accentuates this metabolic heterogeneity.

While multiple hemodynamic and metabolic parameters can now be measured in vivo using PET, there has been much discussion as to which cerebral parameter or parameters best reflects tissue viability. CBF has been found to be quite variable, and in fact may initially be increased even in cases of complete infarction [26–28]. OEF has been examined, and as a general rule, an increase in the oxygen extraction may signify viable tissue [4]. However, since the OEF is calculated on the basis of the ratio of the CO_2 and O_2 images, it may appear falsely elevated whenever CBF is more severely affected than $CMRO_2$ in a pathologic situation [29]. $CMRO_2$ has been cited by some as the best single indication of tissue viability, and levels of oxygen metabolism below which cerebral tissue cannot survive have been suggested [4, 30, 31]. However, $CMRO_2$ will be underestimated in areas of heterogeneous flow; and underestimation of either CBF or OEF without a compensatory increase in the other will result in an underestimation of calculated $CMRO_2$ [29]. These findings in previous studies are in keeping with the results seen in this case, in which no significant global changes in CBF, OEF, or $CMRO_2$ were seen.

A greater than 40% increase in the LCMRGl values was seen on the second study as compared with the first study, with the pretreatment values at the lower limit of the normal range. Owing to the frequent upcoupling of oxygenation and energy metabolism, however, LCMRGl values alone have not been thought to be a reliable index of tissue viability [32]. Some investigators [33] have studied the relationship of LCMRGl to other parameters, examining the ratios of $CMRO_2$ to LCMRGl ("metabolic ratio," MR), and of LCMRGl to CBF ("arteriovenous glucose difference," GLcAv). GlcAv values in that study were quite variable, however, being decreased in 30% of cases and increased in 60% of cases of ischemia [30]. In the present case, greater than 30% increases in GlcAv were seen in both hemispheres after treatment, and approximately 30% decreases in the metabolic ratio were also seen bilaterally. The ratio of CBF to CBV has been suggested as the most reliable predictive parameter of hemodynamic reserve [33]. In our patient, however, no significant overall hemispheric changes in this ratio were seen.

Although the right and left mean hemispheric values of the individual parameters CBV, OEF, and $CMRO_2$ did not change significantly after the treatment, it is interesting to note that a significant decrease in CBV and significant increases in oxygen extraction and in oxygen and glucose utilization were noted in the right parietal region, the posterior watershed area (Table 2), after the endovascular procedures. The change in CBF was not significant in this region, however (<20% increase).

These findings seem to suggest that the improvement in the metabolic parameters studied was most pronounced in the area most severely compromised, the region of arterial border zone where the three vascular territories meet [34]. In this right posterior watershed area, improvement of CBF by less than 20% was sufficient to lead to improvement in the other metabolic parameters. The large change in the GlcAv value in this area reflects a considerable improvement in glucose metabolism with only a modest improvement in CBF. In addition, the change in the CBF/CBV is consistent with the prediction of an improvement in an ischemic state [34].

Overall, the changes in cerebral glucose metabolism and in the LCMRGl/CBF and CBF/CBV ratios correlated most closely with the clinical and angiographic improvements seen. In the area adjacent to the previous ischemic event, and thus the area most severely compromised, significant improvements in multiple metabolic parameters and metabolic ratios were seen. These studies were done at approximately 1 month after the endovascular treatment; additional PET follow-up of this patient may be helpful in evaluating the long-term effects of the procedure.

In summary, Takayasu's disease of the aortic arch can be successfully treated by an endovascular approach. PET performed before and after treatment permits documentation of the improvement of the intracerebral metabolic and hemodynamic parameters.

ACKNOWLEDGMENTS

We thank Peter Ender, Department of Neurology; Jean Talon Hospital, Montreal, for referring this patient to our institute; and Carolyn Elliot for her assistance in the preparation of this manuscript.

REFERENCES

1. Ishikawa K. Natural history and classification of occlusive thromboaorotopathy (Takayasu's disease). *Circulation* **1978**;57:27–34
2. Cooke BE, Evans AC, Fanthome EO, Alarie R, Sendyk AM. Performance figures and images from the Therascan-NS3128 positron emission tomography. *IEEE Trans Nucl Sci* **1984**;31:640–644
3. Diksic M, Jolly D. New high-yield synthesis of ^{18}F-labelled 2-deoxy-2-fluoro-D-glucose. *Int J Appl Radiat Isot* **1983**;34:893–896
4. Frackowiak RSJ, Lensi GL, Jones T. Quantitative measurement of regional cerebral blood flow and oxygen metabolism in man using ^{15}O and positron emission tomography. Theory, procedure, and normal values. *J Cereb Blood Flow Metab* **1980**;4:727–736
5. Lammertsma A, Jones T, Frackowiak R, Lenzi GL. A theoretical study of the steady state model for measuring regional cerebral blood flow and oxygen using oxygen-15. *J Comput Assist Tomogr* **1981**;5:544–550
6. Bergström M, Litton J, Erikson L, Bohm C, Blomquist G. Determination of object contour from projections for attenuation correction in cranial positron emission tomography. *J Comp Assist Tomogr* **1982**;6:365–372
7. Cooke BE, Evans AC. A phantom to assess quantitative recovery of positron tomographs. *J Comput Assist Tomogr* **1983**;7:876–880
8. Strother SC, Thompson CJ, Evans AC. Testing quantitation in PET. *J Nucl Med* **1984**;25:P107
9. Phelps ME, Huang SC, Hoffman EJ, Selin C, Sokoloff L, Kuhl DE. Tomographic measurement of local cerebral glucose metabolic rate in humans with ^{18}F-L-fluoro-2-deoxy-D-glucose; validation of method. *Ann Neurol* **1979**;6:371–388
10. Sokoloff L, Reivich M, Kennedy C, et al. The ^{14}C-deoxyglucose method for the measurement of local cerebral glucose utilization. Theory, procedure, and normal values in the conscious and anesthetized albino rat. *J Neurochem* **1977**;28:897–916
11. Brooks R. Alternative formula for glucose utilization using labelled deoxyglucose. *J Nucl Med* **1982**;23:538–539
12. Huang SC, Phelps ME, Hoffman EJ, Sideris K, Selin CJ, Kuhl DE. Noninvasive determination of local cerebral metabolic rate of glucose in man. *Am J Physiol* **1980**;238:E69–E82
13. Ishikawa K. Survival and morbidity after diagnosis of occlusive thromboaortopathy (Takayasu's disease). *Am J Cardiol* **1981**;47:1026–1032
14. Lande A, Bard R, Bole P, Guarnaccia M. Aortic arch syndrome (Takayasu's arteritis). Arteriographic and surgical considerations. *J Cardiovasc Surg (Torino)* **1978**;19:507
15. Dotter CT, Judkins MP. Transluminal treatment of atherosclerotic obstruction. Description of a new technique and a preliminary report of its application. *Circulation* **1964**;30:654–670
16. Gruntzig A, Hopff H. Percutane rekanalisation kronischer arterieller verschlusse mit einem neuen dilatations katheter. Modification der dotter technik. *Dtsch Med Wochenschr* **1974**;99:2052–2505
17. Hodgins GW, Dutton JW. Subclavian and carotid angioplasties for Takayasu's arteritis. *J Can Assoc Radiol* **1982**;33(3):205–207
18. Martin EC, Diamond NG, Casarella WJ. Percutaneous transluminal angioplasty in non-atherosclerotic disease. *Radiology* **1980**;135:27–32
19. Bockenheimer SA, Mathias K. Percutaneous transluminal angioplasty in arteriosclerotic internal carotid artery stenoses. *AJNR* **1983**;4:791–792
20. Vitek JJ, Raymon BC, Shin JO. Innominate artery angioplasty. *AJNR* **1984**;5:113–114
21. Wiggli V, Gratzl O. Transluminal angioplasty of stenotic carotid arteries. Case reports and protocol. *AJNR* **1983**;4:793–795
22. Bachman DM, Kim RM. Transluminal dilatation for subclavian steal syndrome. *AJNR* **1980**;135:995–996
23. Théron J, Courtheoux P, Henriet JP, Pelouze G, Derlon JM, Maiza D. Angioplasty of supraaortic arteries. *J Neuroradiol* **1984**;11:181–200
24. Motarjememe A, Keifer J, Zuska A, Nabawi P. Transluminal angioplasty in treatment of subclavian steal syndrome. Paper presented at the RSNA meeting, Chicago, **1983**
25. Théron J, Melançon D, Éthier R. Pre-subclavian steal syndromes and their treatment by angioplasty. Hemodynamic classification of subclavian artery stenoses. *Neuroradiology* **1985**;27:265–270
26. Lassen NA. The luxury-perfusion syndrome and its possible relation to acute metabolic acidosis localized within the brain. *Lancet* **1966**;2:1113–1115
27. Pokrupa R, Hakim A, Yamamoto YL, et al. Disturbance of oxygen and glucose metabolism in acute human cerebral infarction studied by positron emission tomography. *Can J Neurol Sci* **1985**;12:179
28. Hakim AM, Pokrupa RP, Diksic M, et al. Acute cerebral infarction in man: studies of cerebral perfusion, metabolism, and acid base status by positron emission tomography. *Ann Neurol* (in press)
29. Wise RSJ, Rhodes CG, Gibbs JM, et al. Disturbance of oxidative metabolism of glucose in recent human cerebral infarcts. *Ann Neurol* **1983**;14:627–637
30. Baron JC, Rougemont D, Bousser MG, Lebrun-Grandié P, Iba-Zizen MJ, Chiras J. Local CBF, oxygen extraction fraction and $CMRO_2$. Prognostic value in recent supratentorial infarction. *J Cereb Blood Flow Metab* **1983**;3:S1–S2
31. Powers WJ, Grubb RL, Raichle ME. Physiological responses to focal cerebral ischemia in humans. *Ann Neurol* **1984**;16:546–552
32. Ackerman RH, Alpert NM, Correia JA, et al. Positron imaging in ischemic stroke disease. *Ann Neurol* **1984**;15:S126–S130
33. Baron JC, Rougemont D, Soussaline F, et al. Local interrelationships of cerebral oxygen consumption and glucose utilization in normal subjects and in ischemic stroke patients. A positron tomography study. *J Cereb Blood Flow Metab* **1984**;4:140–149
34. Russell R. Less common varieties of cerebral arterial disease. In: Russell R, ed. *Vascular disease of central nervous system*, 2nd ed. Edinburgh: Churchill Livingstone, **1983**
35. Gibbs JM, Leenders KL, Wise RJS, Jones T. Evaluation of cerebral perfusion reserve in patients with carotid artery occlusion. *Lancet* **1984**;310–314